The general principle of FTIR spectroscopy is presented in Figure 1.19. The infrared beam coming from the source is directed towards a Michelson interferometer that modulates each wavelength of the beam at a frequency that differs from the frequency associated with IR radiation. In the interferometer, light falls on the lens that splits the beam in two. Half of the beam is directed to a fixed mirror, while the rest is directed to a mobile mirror whose movement modulates the IR beam. When the two beams recombine, destructive or constructive interferences occur, depending on the position of the mobile mirror.

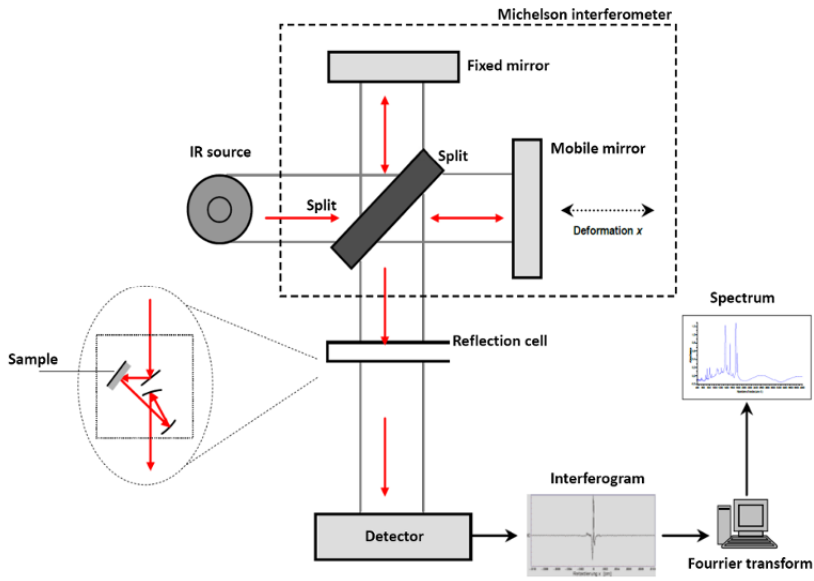

Figure 1.19. *Principle of FTIR spectroscopy, and the cell of measurement in ATR. For a color version of this figure, see www.iste.co.uk/dahoo/metrology1.zip*

The modulated beam is directed towards the sample through a high-index crystal. Absorptions occur in the material in contact with the crystal following an internal reflection and a tunnel effect at the reflection surface. After reflection, the beam returns to a sensor that emits an electrical signal. The latter appears as an interferogram, which is a signal whose amplitude depends on the position of the mobile mirror. This position is determined from a starting position corresponding to an identical position of the two mirrors on the two arms and which corresponds to a zero-path difference

between the two beams and the interference fringes obtained with a He–Ne laser beam that travels along the same path. The modulation of the IR signal corresponds to the Fourier transform of the IR spectrum.

ATR (Attenuated Total Reflection) is a technique that is adapted to the infrared spectroscopy study of materials that are too absorbing or too thick to be analyzed by transmission. In ATR spectrometry, the sample to be analyzed, in liquid or solid state, in the form of powder or thin film, is maintained against the basis of a crystal with high refractive index n_1. For powders and solid materials, a small press is used to maintain the contact with the crystal lens. The other types of samples must be flat or elastic in order to best fit the shape of the crystal.

If n_2 is the refractive index of the sample, there is a total reflection of the incident ray if the angle θ between the sample–crystal interface and the crystal facets is greater than the critical angle θ_c given by the relation: $\sin \theta_c = n_2/n_1$. A certain penetration of the infrared beam takes place at the surface of the sample leading to a decrease in the intensity of the reflected beam in the ranges of frequency where the sample features an absorption. The refractive indices of ATR crystals normally range between 2.4 (ZnSe, KRS-5: mixed crystals of thallium bromides and iodides) and 4 (Ge), and the incidence angles of the systems are generally 30°, 45° and 60°. The total optical path depends on the number of internal reflections, which in turn depends on crystal geometry: length, thickness and angle of incidence.

Using a Thermo Scientific Nicolet iS10 FTIR spectrometer with a Thermo Scientific Smart iTR attenuated total reflectance (ATR) sampling accessory, samples are characterized [KHE 14]. The results in Figure 1.20 correspond to the measurements in the spectral region between 500 and 4,000 cm^{-1} with a resolution of 1 cm^{-1} on various solutions studied in [KHE 14] and whose ellipsometry studies are presented in Chapter 8 of [DAH 16].

The same peaks are found on the spectra of all polymers. The valence vibrations of methyl groups are observed for the CH stretching mode in the form of a group of about 2,962 cm^{-1} and 2,904 cm^{-1}; the stretching vibrations are about 1,413 cm^{-1} followed by a small band at 14,40 cm^{-1}. The antisymmetric stretching of siloxane Si–O–Si functions, which have the

form of a high peak with a shoulder, is about 1,008 cm^{-1} and 1,082 cm^{-1}. Si–C valence vibrations have the form of a very high peak about 784 cm^{-1} corresponding to the rocking stretching of $Si–CH_3$, a stretching mode at 864 cm^{-1} and a significant band at 1,258 cm^{-1} corresponding to a stretching vibration. The seven samples from different suppliers have the same spectral signature, the only difference being absorption intensities and an additional band for M2. The difference in intensity between the absorption peaks reflects a difference in the concentration of functional groups specific to each supplier in the polymer chain.

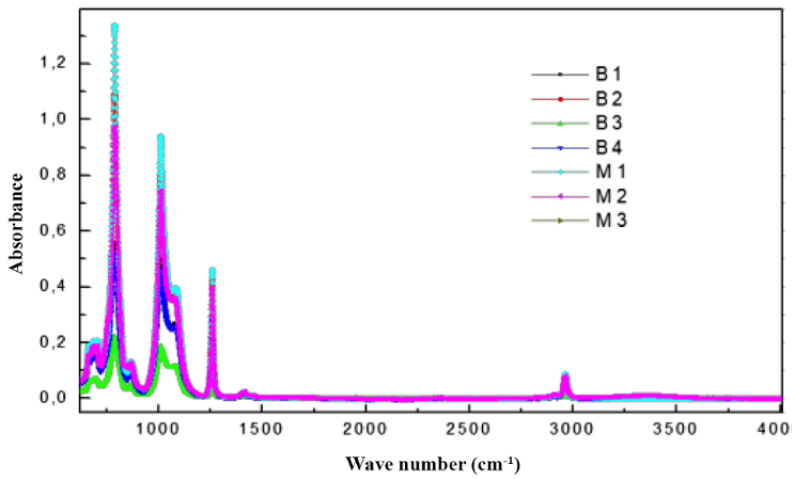

Figure 1.20. *Absorption spectra of silicone gels B (1–4) and M (1–3). For a color version of this figure, see www.iste.co.uk/dahoo/metrology1.zip*

An ATR spectroscopy study of polymers is conducted on samples of polymer subjected to constraints of temperatures and humidity in a super-Highly Accelerated Life Test (HALT) and Highly Accelerated Testing (HAT) device described in Chapter 1 of [POU 20]. Among the characteristics of HALT, which comprises a generator of vibrations and thermal shocks, the following can be listed: a T° slope of 60°/mn, a range of T° between +200° and -100°C and a range of vibration per pistons under the lower plate between 0 and 50 g. The humidity generator can reach a maximal relative humidity of 98%, for a volume of 1,680 liters. To run the aging tests, the test profile software control in terms of temperature, vibration and humidity is activated. The polymer samples were subjected to cycles such as those represented in Figures 1.20 and 1.21.

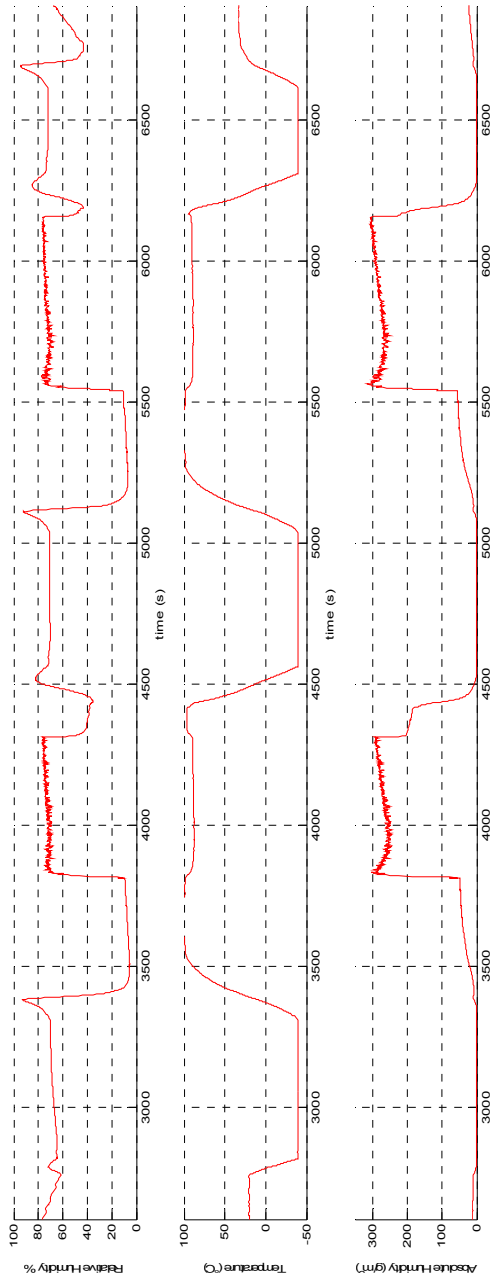

Figure 1.21. *Combined thermal cycling (T: -45 at 95°C) and humidity cycling (HR: 70%) in the super-HAT. For a color version of this figure, see www.iste.co.uk/dahoo/metrology1.zip*

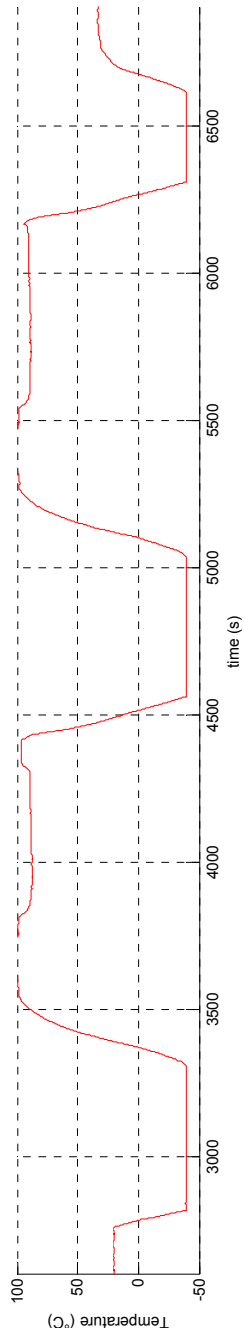

Figure 1.22. *Thermal cycling (T: -45 at 95°C) in HALT. For a color version of this figure, see www.iste.co.uk/dahoo/metrology1.zip*

To study the effect on aging of an environment combining relative humidity with temperature, two types of loads are applied: a (T+H) load (Figure 1.21) combining a temperature cycle (variation of temperature between 45°C and 95°C) with a humid atmosphere (maximum relative humidity rate is 78%) and a (THalt) load consisting of thermal cycles (Figure 1.22).

Another type of aging due to a more classical aggressive thermal stress is conducted on polymers in a furnace. The various stress temperatures are 150°C, 180°C and 200°C. The monitored thermal profile is programmed by a progressive increase in temperature from 25°C to the temperature to be reached during 15 minutes followed by a plateau of 2 h at this temperature. All the samples are subjected to the same process under the same conditions. Figure 1.23 displays the applied thermal cycles.

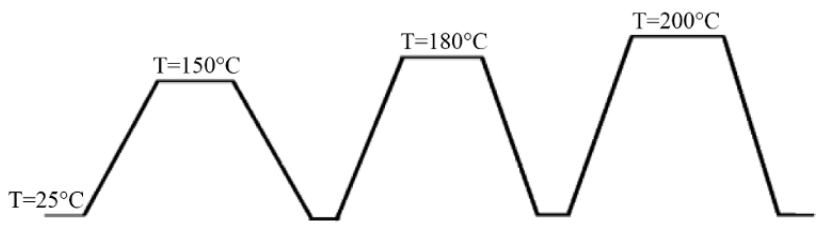

Figure 1.23. *Thermal cycling in a furnace*

The spectra were obtained by ATR in the interval between 600 cm^{-1} and 4,000 cm^{-1}. The analyses show a differentiation in the results in two different spectral regions located between 600 cm^{-1} and 1,500 cm^{-1} and between 2,280 cm^{-1} and 2,400 cm^{-1}. The first interval corresponds to the region of Si–O vibration modes and the second interval to the spectral signature of CO_2 vibration modes, indicating the presence of this molecule that is trapped in nanocages in the polymer structure.

Figure 1.24 shows the spectra obtained with M-type polymers (1 component). Figure 1.25 shows the spectra obtained with B-type polymers (2 components) in the region of Si–O, between 600 cm^{-1} and 1,500 cm^{-1}. The spectra are denoted by {TF} for the thermal stress applied in a furnace, {Thalt} for the thermal stress in a dry environment and {T+H} for the thermal stress in a humid environment.

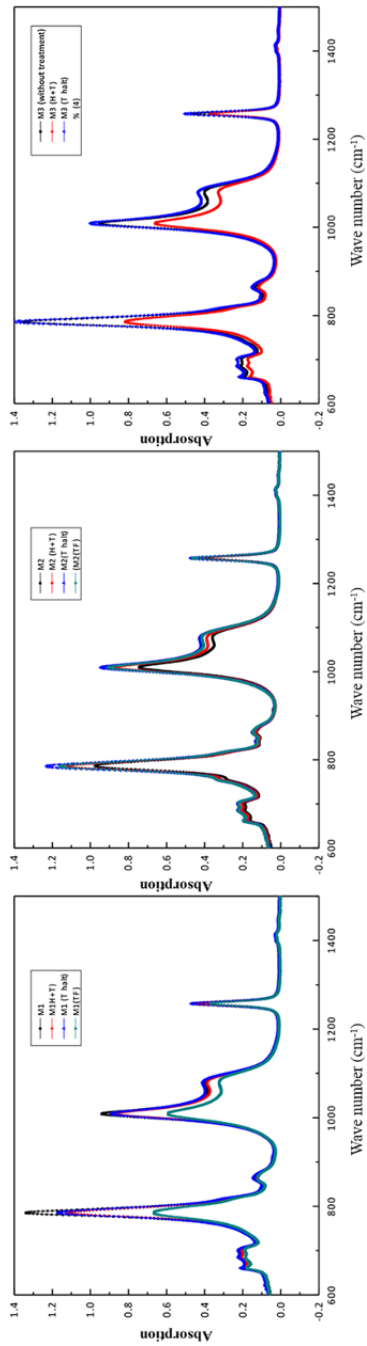

Figure 1.24. *ATR spectra of M-type polymers. For a color version of this figure, see www.iste.co.uk/dahoo/metrology1.zip*

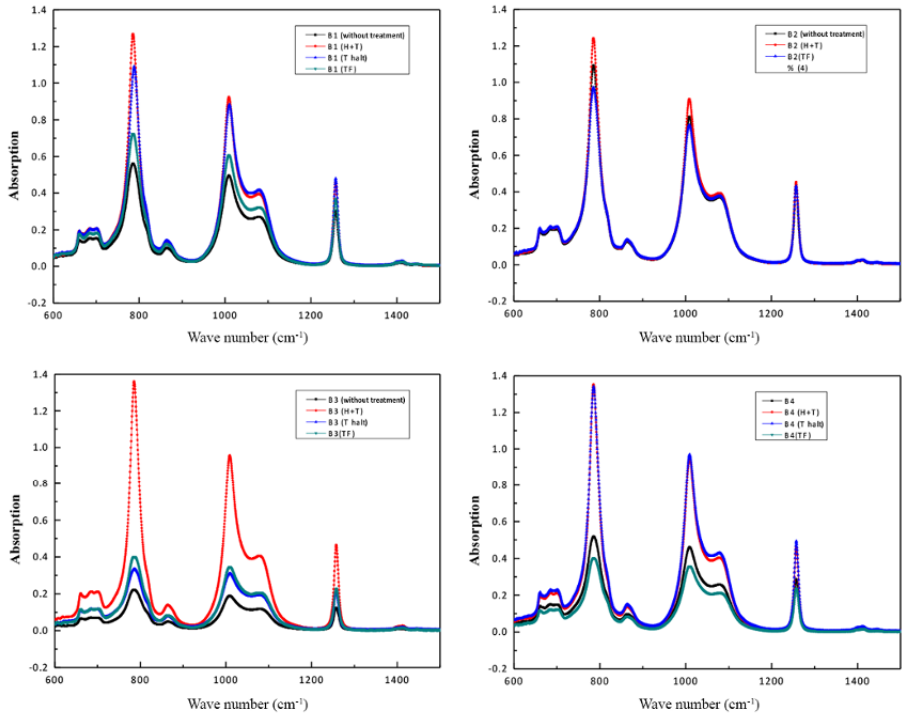

Figure 1.25. *ATR spectra of B-type polymers. For a color version of this figure, see www.iste.co.uk/dahoo/metrology1.zip*

The intensities of absorption peaks vary for each material, but in different proportions. The absorption increases or decreases depending on the material and the TF, THalt or {T+H} loads. As a general rule, the increase or decrease in the intensity of an absorption peak by thermal processing influences also all the peaks of the spectrum in the same direction of variation. Either an increase or a decrease in the intensity can be observed throughout the spectrum, but observing a decreasing peak and an increasing peak and vice versa is excluded. No general tendency of evolution of the intensities of absorptions depending on the thermal processing can be globally established.

The effect on the spectral signatures of {THalt} and {T+H} loads is more or less similar in the two groups of M-type or B-type polymers. In the B-types, the peaks are rather more intense or of the same order as for the M-type. Comparing the effect of the three thermal processes, the spectral signature of the TF effect corresponds to signals of lower intensity than for {THalt} and {T+H,} effects, with the exception of the two compounds M2 and B2 with equivalent signatures.

Concerning the zone located in the region of intense absorption of the antisymmetric stretching vibration of CO_2, between 2,280 cm^{-1} and 2,400 cm^{-1}, the absorption spectra have the same evolutions in the intensities of the peaks of absorptions before and after processing, independently of each material. This analysis yields different results from those obtained on the spectra from 600 cm^{-1} to 1,500 cm^{-1}. Relying on the intensity of absorption bands centered at 2,350 cm^{-1}, the following characteristics are listed.

All the polymers feature a quasi-null absorption in the IR spectrum at a very low level (Absorbance $\approx$ 0) before the application of the thermal constraint. On the other hand, the thermal load in a humid environment {T+H} leads to an increase in absorbance, contrary to the {THalt} and {TF} loads that lead to a decrease in absorbance (Absorbance < 0).

A study of possible absorptions in this region reveals the absorption by triple bonds (C≡O, C≡N) from 2,000 cm^{-1} to 2,500 cm^{-1}, by double bonds (C=O, C=N and C=C) from 2,000 cm^{-1} to 1,500 cm^{-1} and more specifically, the case of a double bond (O=C=O) as in CO_2. For the latter, it is worth noting the presence of a vibration–rotation band (Branch P and R) centered in the gaseous phase at 2,349.14 cm^{-1} due to the absorption of the mode of vibration ν_3 of antisymmetric stretch of CO_2. This corresponds with the identified zone taking into account the effect of nanocage perturbation [DAH 99, DAH 06] on the motion of the molecule as a result of the interaction with the electrical field present in the polymer. In order to evidence the presence of CO_2 in the polymers, the difference spectra are drawn using the spectrum recorded after applying the most aggressive thermal load {TF} as a basic line. The curves are represented in Figures 1.26 and 1.27 for type M and B polymers, respectively.

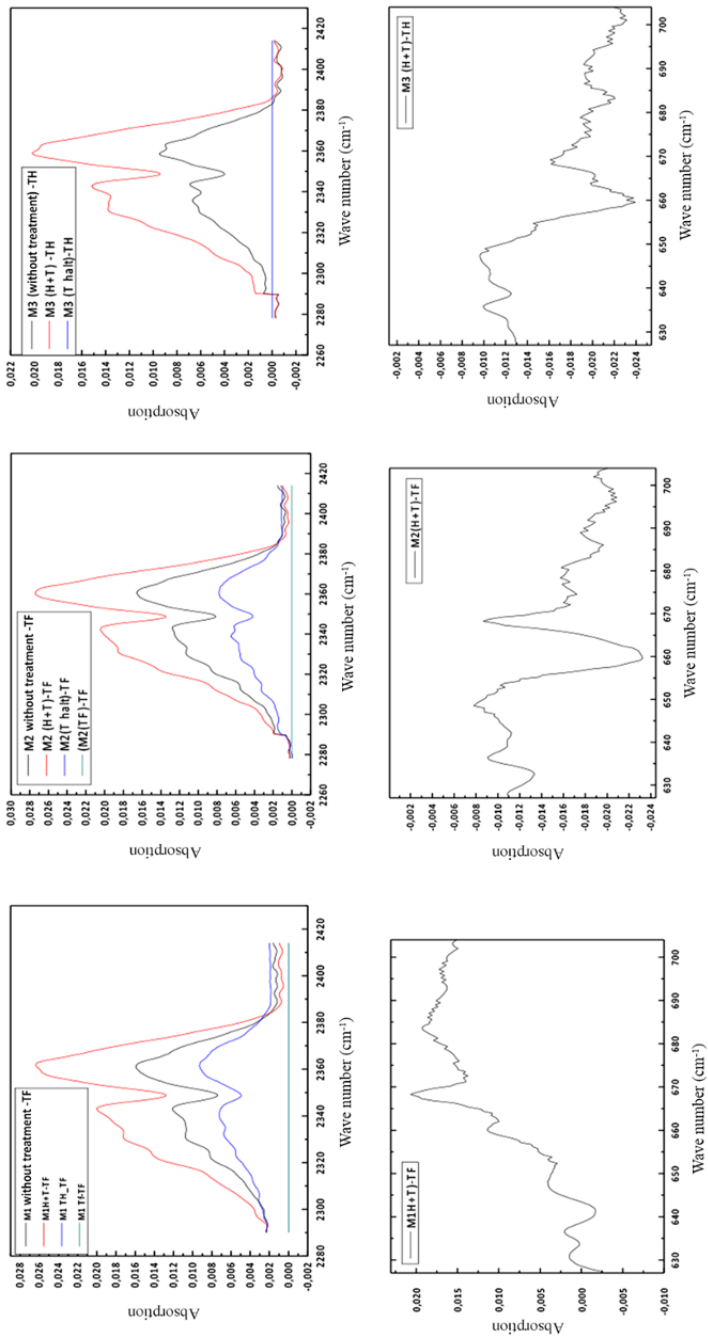

Figure 1.26. *ATR difference spectra for M-type polymers. For a color version of this figure, see www.iste.co.uk/dahoo/metrology1.zip*

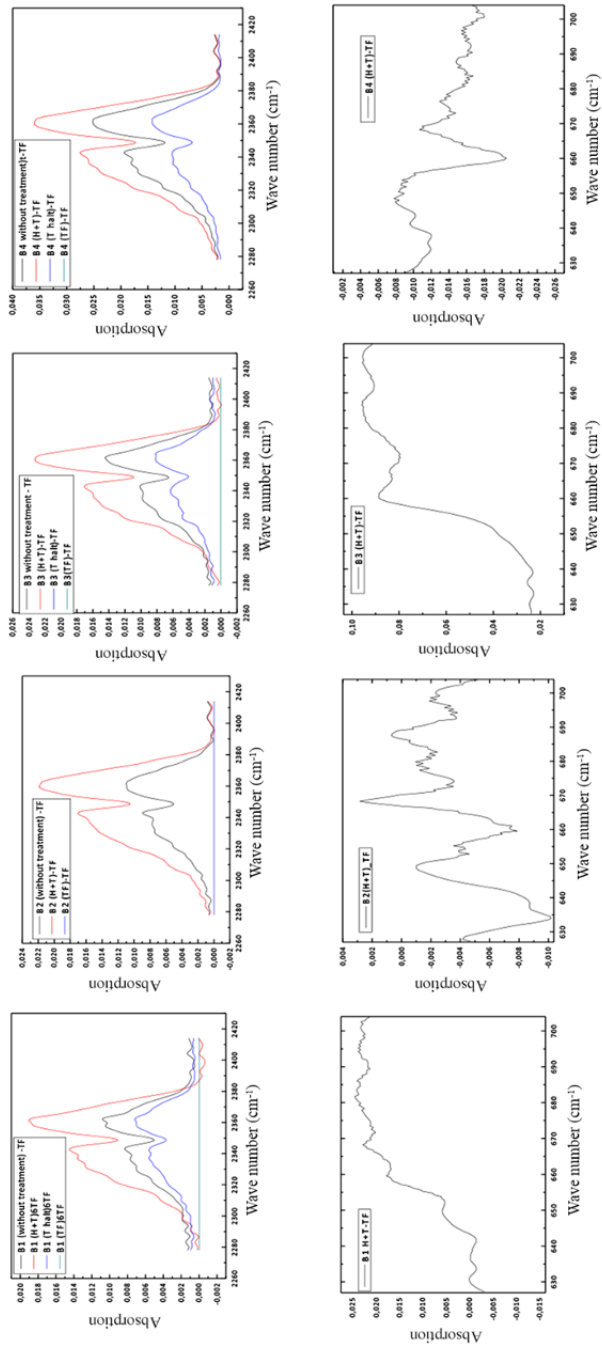

Figure 1.27. *ATR difference spectra for B-type polymers. For a color version of this figure, see www.iste.co.uk/dahoo/metrology1.zip*

The difference spectra clearly show the absorptions of CO_2 in the region of absorption in the band associated with the antisymmetric stretching approximately 2,350 cm^{-1} characterized by a branch P (low frequency) and a branch R (high frequency). The gap between the maximum of each branch is about 22 cm^{-1}. This gap is given by the formula $\Delta\nu = 2,358\sqrt{TB}$ [HER 45], where $\Delta\nu$ is expressed in cm^{-1}, B is the rotational constant of CO_2 and T is the absolute temperature. Considering a value of 0.39 cm^{-1} for B and 293 K for T, a gap of 25 cm^{-1} is calculated, which is comparable to the value measured on the spectra. In the region of atmospheric absorption of the bending mode band ν_2, the peak at 668 cm^{-1} can be observed, particularly on M-type polymers. This value can be compared with that of 667 cm^{-1}, which corresponds to the absorption in gaseous phase of this vibration that is doubly degenerate. Certain spectra feature a doublet at 650 cm^{-1}, 655 cm^{-1}, which might be associated with a degeneracy removal.

CO_2 could be simultaneously considered a Lewis acid (positive charge on the central carbon, electron acceptor) and a Lewis base (negative charge on the terminal oxygen atoms, electron donors). According to the works conducted on CO_2 in polymers [NAL 05, NAL 06, CUL 13], degeneracy removal is due to an interaction of the type Lewis acid–base between CO_2 and the groups in the polymer (ester, ether, aromatic ring, carbonyl group, etc.). Degeneracy removal is due to interactions with the carbonyl group, aromatic rings or sites with basic properties.

1.4. Conclusion

This chapter presents various deposition techniques that are used for material nano-structuring, as well as the equipment developed for sample characterization and analysis. In situ during the elaboration phase, these techniques are used to control the fabrication of materials on the nanometer scale. Some of these techniques can be used to manipulate matter at the scale of atoms. A detailed study using ATR spectroscopy, through which a material is probed by the tunnel effect over a nanometer-scale thickness, is presented. The material being pressed firmly into contact on a high-index crystal, the beam returning after total reflection is used to obtain an IR beam containing information on the spectral signature of the constituents trapped in the polymer. Absorption of CO_2 is revealed in the polymers used as encapsulation material.

1.5. Appendix: light ray propagation

In light diffraction problems, the amplitude of a wave $E_z(x,y)$ on a surface located in a plane z is determined from the amplitude $E_0(x,y)$ of a wave in the plane z = 0.

In Chapter 3 of [DAH 16], equation 3.6 gives the expression of an electromagnetic wave moving along Oz, in the form u (z-vt) = acos (k(z-ct)), where v is the wave propagation speed in a medium of index n, a its amplitude and k = 2 πn/λ. In a vacuum, n = 1 and in a three-dimensional space, the monochromatic plane wave of angular frequency ω = kc and of wave vector **k** = (kx, ky, kz) can be expressed in complex notation, in the form $\mathbf{E} = \mathbf{E_0} \exp i(2\pi/\lambda\ (\alpha x+\beta y+\gamma z) - \omega t)$, where the components of the wave vector are in the form $k_x = 2\pi\alpha/\lambda$, $k_y = 2\pi\beta/\lambda$ and $k_z = 2\pi\gamma/\lambda$, with α, β and γ being the direction cosines of the wave vector **k** and λ the wavelength. This expression can be obtained by solving the Helmholtz equation (equation 3.7, [DAH 16]):

$$\Delta\vec{\mathrm{E}} + \frac{\omega^2}{c^2}\vec{\mathrm{E}} = \vec{0} \qquad [1.1]$$

where $\Delta\vec{\mathrm{E}} = \vec{\nabla}^2\vec{\mathrm{E}}$, using the Green function $G_k(\vec{r},\vec{r}_0)$ of the Helmholtz equation, which verifies that:

$$(\nabla^2 + \mathrm{k}^2)G_k(\vec{r},\vec{r}_0) = \delta(\vec{r} - \vec{r}_0) \qquad [1.2]$$

given that: $G_k(\vec{r},\vec{r}_0) = -\frac{exp(ik|\vec{r}-\vec{r}_0|)}{4\pi|\vec{r}-\vec{r}_0|}$, and the unit vector $\vec{e}_r = \frac{(\vec{r}-\vec{r}_0)}{|\vec{r}-\vec{r}_0|}$. The solution is straightforward, and for the k mode of the electric field from a source placed in $\vec{r}_0$, we can write: $\vec{E}_k(\vec{r},\vec{r}_0) = -\frac{exp(ik|\vec{r}-\vec{r}_0|)}{4\pi|\vec{r}-\vec{r}_0|}\vec{e}_r$.

The propagation of a wave through objects (transparent apertures or opaque objects) can be determined using the Green–Ostrogradsky theorem and the Green function $G_k(\vec{r},\vec{r}_0)$ of the Helmholtz equation.

From the relation:

$$\vec{\nabla}\left(u\vec{\nabla}\mathrm{v} - \mathrm{v}\vec{\nabla}\mathrm{u}\right) = u\vec{\nabla}^2 v - v\vec{\nabla}^2 u = u\Delta v - v\Delta u \qquad [1.3]$$

where u and v are solutions of the Helmholtz equation, and from the Green–Ostrogradsky theorem, which transforms a volume integral into a surface integral:

$$\int (u\Delta v - v\Delta u)d\tau = \int \left(u\vec{\nabla}^2 v - v\nabla^2 u\right)d\tau = \oint \left(u\vec{\nabla}\mathrm{v} - \mathrm{v}\vec{\nabla}\mathrm{u}\right)d\vec{s} \qquad [1.4]$$

It can be written that:

$$\int \left(\vec{\mathrm{E}}(\vec{r})\Delta G_k(\vec{r},\vec{r}_0) - G_k(\vec{r},\vec{r}_0)\Delta\vec{\mathrm{E}}(\vec{r})\right)d\tau = \int \vec{\mathrm{E}}(\vec{r})\delta(\vec{r}-\vec{r}_0)d\tau$$

$$-\int \vec{\mathrm{E}}(\vec{r})\mathrm{k}^2 G_k(\vec{r},\vec{r}_0)d\tau + \int G_k(\vec{r},\vec{r}_0)\mathrm{k}^2\vec{\mathrm{E}}(\vec{r})d\tau = \vec{\mathrm{E}}(\vec{r}_0) \qquad [1.5]$$

Hence

$$\vec{\mathrm{E}}(\vec{r}_0) = \oint \left(\vec{\mathrm{E}}(\vec{r})\vec{\nabla}G_k(\vec{r},\vec{r}_0) - G_k(\vec{r},\vec{r}_0)\vec{\nabla}\vec{\mathrm{E}}(\vec{r})\right)d\vec{s} =$$
$$\oint\left(\vec{\mathrm{E}}(\vec{r})\left\{\vec{\nabla}G_k(\vec{r},\vec{r}_0)d\vec{s} - ikG_k(\vec{r},\vec{r}_0)ds\right\}\right) \qquad [1.6]$$

where the surface integral bounds the point located at $\vec{r}_0$ and $\vec{r}$ is the position vector of the surface element $d\vec{s}$ (Figure 1.28), such that $\vec{\nabla}\vec{\mathrm{E}}(\vec{r}).d\vec{s} = ik\vec{\mathrm{E}}(\vec{r})ds$, for a wave that propagates inwards in the volume bounded by the integral surface element ds. For a wave propagating outwards of the surface, $\vec{\mathrm{E}}(\vec{r}).d\vec{s} = -ik\vec{\mathrm{E}}(\vec{r})ds$.

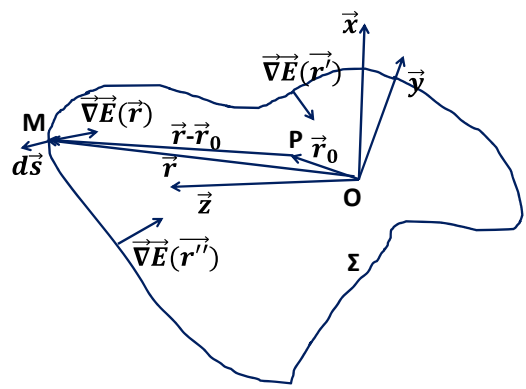

Figure 1.28. *Kirchhoff integral on a surface Σ passing through a point M enclosing the point P. For a color version of this figure, see www.iste.co.uk/dahoo/metrology1.zip*

Given that $G_k(\vec{r},\vec{r}_0) = -\frac{exp(ik|\vec{r}-\vec{r}_0|)}{4\pi|\vec{r}-\vec{r}_0|}$, it can be written that:

$$\vec{\nabla}G_k(\vec{r},\vec{r}_0) = ikG(\vec{r},\vec{r}_0)\vec{e}_r + \frac{exp(ik|\vec{r}-\vec{r}_0|)}{4\pi|\vec{r}-\vec{r}_0|^2}\vec{e}_r = \left(\frac{ik}{|\vec{r}-\vec{r}_0|} - \frac{1}{|\vec{r}-\vec{r}_0|^2}\right)(\vec{r} - \vec{r}_0)G_k(\vec{r},\vec{r}_0) \quad [1.7]$$

At a great distance compared to the wavelength such that $k|\vec{r}-\vec{r}_0| \gg 1$, the following solution is obtained:

$$\vec{\mathrm{E}}(\vec{r}_0) = \oint\left(\vec{\mathrm{E}}(\vec{r})\left\{\frac{ik}{|\vec{r}-\vec{r}_0|}(\vec{r}-\vec{r}_0)G_k(\vec{r},\vec{r}_0)d\vec{s} - ikG_k(\vec{r},\vec{r}_0)ds\right\}\right) \quad [1.8]$$

such that:

$$\vec{\mathrm{E}}(\vec{r}_0) = -\frac{ik}{4\pi}\oint\vec{\mathrm{E}}(\vec{r})\frac{exp(ik|\vec{r}-\vec{r}_0|)}{|\vec{r}-\vec{r}_0|^2}\left((\vec{r}-\vec{r}_0)d\vec{s} - |\vec{r}-\vec{r}_0|ds\right) \quad [1.9]$$

This solution is the mathematical formulation of the Huygens–Fresnel principle or the Huygens–Fresnel equation obtained by the Kirchhoff integral. Hence, it is the Fresnel–Kirchhoff diffraction formula.

When a monochromatic plane wave propagating parallel to Oz encounters a screen (E_0) with an opening (Figure 1.29), a diffraction pattern is formed in the observation plane. To simplify, the plane of the opening is supposed to be perpendicular to the propagation of the plane wave and that the amplitude and the gradient of the electric field of the wave are constant on the surface of the opening located in the vicinity of M (Figure 1.28) and zero elsewhere. The amplitude on the other side of the aperture at a point P located at $\vec{r}_0$ is given by the Fresnel–Kirchhoff diffraction formula. If the opening is in the Oxy plane (Figure 1.29), and the dimensions are small compared to the position of the point P located at $\vec{r}_0$, the amplitude of the field at P writes as:

$$\vec{\mathrm{E}}(\vec{r}_0) = -\frac{ik\vec{\mathrm{E}}(\vec{r})}{4\pi R}(cos\theta + 1)\oint exp(ik|\vec{r}-\vec{r}_0|)dxdy \quad [1.10]$$

where R is the distance between the center of the opening and the point P (as a first approximation, it is the same distance for all the points of the opening), and θ is the angle between the axis Oz and the vector $\overrightarrow{MP} = \vec{r}_0 - \vec{r}$. The origin of the coordinates system is the plane containing the diffracting opening.

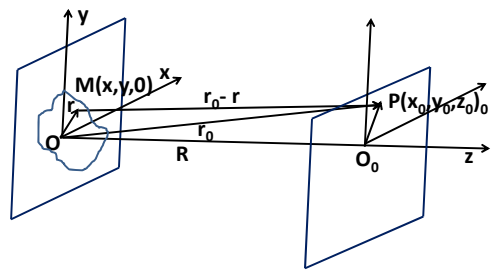

Figure 1.29. *Schematic of the diffraction by an aperture scanned by M in a plane at point P. For a color version of this figure, see www.iste.co.uk/dahoo/metrology1.zip*

The modulus of vector $\vec{r}_0 - \vec{r}$ is given by: $|\vec{r}_0 - \vec{r}| = \sqrt{r_0^2 - 2\vec{r}_0.\vec{r} + r^2}$.

Under the far-field Fraunhofer diffraction conditions, with an origin O in the plane of the aperture (Figure 1.29), where R is the distance between the observation plane and the diffracting plane, we can write that:

$$exp(ik|\vec{r} - \vec{r}_0|) = exp\left(ik\sqrt{r_0^2 - 2\vec{r}_0.\vec{r} + r^2}\right)$$
$$= e^{ikR}exp\big(-ik(\alpha x + \beta y)\big) \qquad [1.11]$$

where: $\alpha = \frac{x_0}{R}$ and $\beta = \frac{y_0}{R}$.

In the case of the Gaussian approximation, with paraxial light rays, the field at P is expressed as:

$$\vec{E}(\vec{r}_0) = A \iint exp\big(-ik(\alpha x + \beta y)\big)dxdy \qquad [1.12]$$

We can thus calculate the Fraunhofer diffraction at a far distance by this formula. In the case of a circular aperture, it can be written as:

$$\vec{E}(\vec{r}_0) = A \iint exp\big(-ik(\alpha\rho cos\varphi)\big)\rho d\rho d\varphi$$

$$= 2\pi A \int_0^a J_0(k\alpha\rho)\rho d\rho = 2\pi A a^2 \frac{J_1(k\alpha\rho)}{k\alpha\rho} \qquad [1.13]$$

where $J_0(x)$ and $J_1(x)$ are the Bessel functions of zeroth and first orders, respectively.

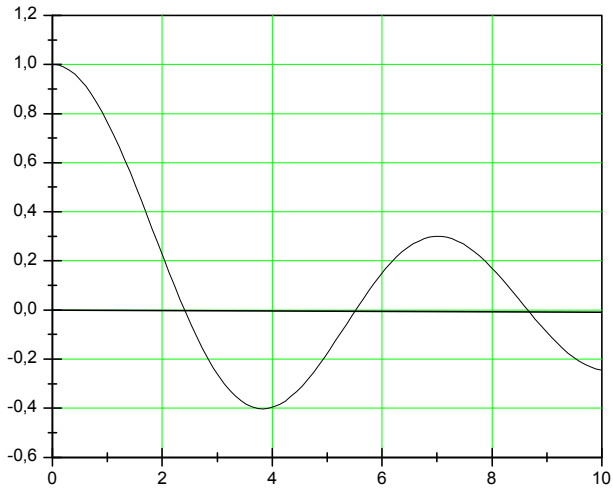

Figure 1.30. *Diffraction amplitude distribution by a circular aperture. For a color version of this figure, see www.iste.co.uk/dahoo/metrology1.zip*

Fresnel diffraction is localized in an observation plane closer to the aperture than a distance of $\lambda/2\pi$. In this case, the terms of order 2 in x and y must be considered and it is wise to use a coordinate system so as to get rid of the terms of order 1 in x and y. The aperture is placed in the Oxy plane with the Oz axis, which is perpendicular to the plane passing through the observation point r_0. In this coordinate system, $\alpha = \beta = \vec{r}.\vec{r}_0$=0. Under such conditions, the following expression is calculated:

$$exp(ik|\vec{r} - \vec{r}_0|) = exp\left(ik\sqrt{r_0^2 - 2\vec{r}_0.\vec{r} + r^2}\right) = e^{ikR} exp\left(\frac{ik(x^2+y^2)}{2R}\right) \quad [1.14]$$

In the case of the Gaussian approximation, with paraxial light rays, the field at P is expressed as:

$$\vec{E}(\vec{r}_0) = A \int exp\left(\frac{ikx^2}{2R}\right) dx \int exp\left(\frac{iky^2}{2R}\right) dy \quad [1.15]$$

From which it is possible to calculate the Fresnel diffraction pattern.

2

Statistical Tools to Reduce the Effect of Design Uncertainties

The inclusion of the ability to resist potential design or process variations is an innovative product design approach. This includes managing critical parameters of the system, using security coefficients and applying more advanced techniques for reliability optimization. This approach consists of applying statistics to design a system that has the best performance although its parameters have potential variations. The designed product respects the required performance in spite of uncertainties and remains above a threshold of minimal performance for a given probability. These innovative engineering design methods are related to multi-objective optimization problems. This chapter presents several methods and practical applications for improving the system design by including potential uncertainties.

2.1. Introduction

When a product is mass manufactured, it is obvious that design parameters must respect both manufacturing tolerances and expected variable final use conditions. The corresponding unknown parameters must be taken into account during product design. The statistical tools that include system uncertainties rely on:

– developing an approximate mathematical model of the physical system under study;

– identifying and characterizing the sources of uncertainty among the parameters of the model;

Applications and Metrology at Nanometer Scale 1:
Smart Materials, Electromagnetic Waves and Uncertainties,
First Edition. Pierre-Richard Dahoo, Philippe Pougnet and Abdelkhalak El Hami.

– studying the propagation of uncertainties and their impact on the output signal (response) of the system.

The methods for propagation of uncertainties depend on the mathematical tools that are used. The principal methods applied are the reliability-based design optimization, the probabilistic approach based on design of experiments and the set-based approach. A post-processing stage offers the possibility of analyzing and statistically characterizing the response (statistical moments, distribution, etc.).

2.2. Review of fundamental definitions in probability theory

2.2.1. *Definitions and properties*

Fundamental definitions of the probability theory are presented [MOH 10].

Consider a domain D that represents the physical domain on which the problem is defined.

In addition, consider the space H of real-valued functions defined over D:

$$H=\{ f \ /f: D \rightarrow \mathbf{R} \}$$

The inner product over H is defined as:

$$\langle f(x), g(x) \rangle = \int_D f(x).\overline{g(x)}dx \qquad [2.1]$$

where $f, g \in$ H and g^* is the complex conjugate of g.

With this scalar product, H is a Hilbert space.

The probability theory seeks to formally model intrinsically random phenomena using random experiments.

A random experiment ε is fully described by the probability triplet (Ω, B, p), which is also referred to as "the probability space associated with the random experiment ε".

Ω: is a random set that represents the set of all possible results of the experiment ε.

B: is the set of events of ε (also known as σ-algebra in the analysis).

p: is the probability defined on (Ω, *B*).

Therefore, a probability is defined on an arbitrary set Ω associated with a set *B* of partitions of Ω, which verifies the following properties:

i) $\Omega \in B$.

ii) If $A \in B$, then $\overline{A} \in B$ ($\overline{A}$ is the complementary of "*A*").

iii) Any finite or countable union of elements of *B* belongs to *B* $A_j \in B, \forall j \in N \rightarrow \bigcup_{j=0}^{+\infty} A_j \in B$ and $\bigcap_{j=0}^{+\infty} A_j \in B$.

Hence, the probability of p on (Ω, *B*) is an application of *B* in [0,1], which verifies that:

$$\begin{cases} p(\Omega) = 1 \\ p\left(\bigcup_{j \in J} A_j\right) = \sum_{j \in J} p(A_j) \end{cases} \qquad [2.2]$$

for any finite countable set of disjoint events $(A_j, j \in J)$, i.e. for any A_j such that: $A_j \cup A_k = \phi \quad \forall (A_j, A_k) \in \Re^2, j \neq k$.

Consequently, for arbitrary events A and B, we have the following properties:

i) $p(\phi) = 0$

ii) $p(A) = 1 - P(\overline{A})$

iii) $p(A \cup B) = p(A) + P(B) - P(A \cap B)$ [2.3]

iv) $A \subset B \Rightarrow p(A) \leq p(B)$

v) $p(A \cap B) \leq P(A) \leq p(A \cup B)$

Let (Ω, B, p) be a probability space. The space Θ of real-valued measurable functions of Ω is defined as:

$$\Theta = \{g / g : \Omega \rightarrow \Re\}$$

The inner product on Θ is defined similarly to the inner product of H:

$$\langle \alpha(\theta) \beta(\theta) \rangle = \int_{\Omega} \alpha(\theta) \beta(\theta) \, dp, \alpha, \beta \in \Theta \qquad [2.4]$$

2.2.2. *Random variables*

A real random variable X is a B-measurable application of Ω in $\Re$, which means that for any A $\in B(\Re)$, a Borel set, we have $X^{-1}(A) \in B$. The application X generates a probability P_X on $(\Re, B(\Re))$, which is defined as:

$$P_X(A) = p\left[X^{-1}(A)\right] = p[\omega \in \Omega, X(\omega) \in A] \qquad [2.5]$$

Here "X" is related to a random experiment whose results are real numbers.

Hence, $P_X(A)$ is the probability that the result of the experiment belongs to A.

In the case of discrete random variables, the probability law of X is defined as:

$P(X = x_j) = P_j$, $j \in J$; J finite countable.

where $P_j > 0$ and $\sum_{j \in J} P_j = 1$; with $x_j \neq x_k$ for $j \neq k$.

$$p(X \in A) = \sum_{j:x_j \in A} p_j$$

For a continuous random variable, the probability law of X is defined by a probability density function $f(x)$ such that:

$$p(X \in A) = \int_A f(x)dx \qquad [2.6]$$

and $\forall x \in \Re \quad f(x) \geq 0 \quad$ and $\quad \int_{-\infty}^{+\infty} f(x)\,dx = 1 \qquad [2.7]$

2.2.3. *Random vectors*

A real (or complex) random vector $\{X\}$ of size "*n*" on the set Ω is defined as a function of Ω for x, the subspace of $\Re^n$ (or C^n):

$$\{X\}(w) : \Omega \rightarrow x \subset \Re(or\ C)$$

The real random vector $\{X\}$ is a vector of "*n*" real random variables:

$$\{X\} = \{X_1, X_2, \ldots, X_n\}^T$$

The function $\{X\}(w)$ must verify the following conditions:

a) The set $\{w : \{X\}(w) \leq \{x\}\}$ is an event in Ω for $\forall \{X\} \in \Re^n$.

(The notation $\{X\}(w) \leq \{x\}$ means that, for any *i*=1,2,……,*n*, we have $X_i(w) \leq x_i$);

b) $p(\{w : \{X\}(w) \leq +\infty\}) = 1$;

c) $p(\{w:\{X\}(w)\leq-\infty\})=0.$

The definitions of the probability density function can be extended to vectors of random variables.

Hence, we define the joint probability function of order n, denoted by $f_n(x_1,x_2.....,x_n)$, for a vector of random variables $\{X\}$ of size "n", such that:

$$p(a_i \leq x_i \leq b_i) = \int_a^b \int_{a_2}^{b_2} ..... \int_{a_n}^{b_n} f_n(x_1, x_2, ...x_n) d_1 dx_2 .....dx_n$$

With the properties:

$$f_n(x_1,x_2.....x_n) \geq 0$$
$$\underbrace{\int_{-\infty}^{+\infty}\int_{-\infty}^{+\infty}\cdots\cdots\int_{-\infty}^{+\infty}}_{n\ times} f_n(x_1, x_2, ...x_n) = 1 \qquad [2.8]$$

where $p(a_i \leq x_i \leq b_i)$ is the probability that the random variable X_i ranges between a_i and b_i.

2.2.4. *Static moments*

The moments of one or several random variables are defined as the mathematical expectations of various powers of these random variables. For a single variable, $E[X^n]$ is the moment of order "n"; $E[X^m Y^n]$ is the joint moment of order "m + n" of variables "X" and "Y". Once the probability distribution is known, all the moments can be calculated.

However, without additional information (as is the case for a normal distribution), knowing the moments of all the orders is a prerequisite for obtaining the probability distribution.

If $Y = g(x)$ is a continuous and real function of the random variable X, then Y is also a random variable, and the mathematical expectation of the function $g(X)$ is defined as:

$$E[Y] = E[g(X)] = \int_{-\infty}^{+\infty} g(x) f(x) dx \qquad [2.9]$$

where $f(x)$ is the probability density function of the variable X.

In the specific case of $g(X) = x$, the mathematical expectation $E[g(X)]$ becomes the *expected or mean value* of the random variable X, denoted by $\mu(X)$ or $\bar{x}$, such that:

$$\mu(X) = \int_{-\infty}^{+\infty} x f(x) dx \qquad [2.10]$$

Generally speaking, we can define the K-th static moment of a random variable as:

$$\mu^k(X) = \int_{-\infty}^{+\infty} x^k f(x) dx \qquad [2.11]$$

The centered static moments are defined with respect to the mean:

$$\overline{\mu^k}(X) = E[(X - \mu(X))^k] = \int_{-\infty}^{+\infty} (x - \bar{x})^k f(x) dx \qquad [2.12]$$

The first static moment is the mean defined by equation [2.11]; the second centered moment defines the variance of the random variable.

The variance of the random variable can be defined as:

$$V(X) E(X^2) + (E(X))^2 \qquad [2.13]$$

PROPERTIES.–

$$E(aX+b)=aE(X)+b$$

$$V(aX+b)=b \qquad [2.14]$$

$$E(X-E(X))=E(X)-E(X)=0$$

$$V\left(\frac{X-E(X)}{\sigma(X)}\right)=1 \qquad [2.15]$$

The variance of a reduced centered variable is equal to 1:

$$E\left(\frac{X-E(X)}{\sigma(X)}\right)=0 \qquad [2.16]$$

The expectation of a reduced centered variable is equal to 1.

The positive root of the variance defines the *standard deviation* of the random variable; *the coefficient of variation* of a random variable is given by:

$$\varsigma(X)=\sqrt{\frac{Var(X)}{\mu(X)^2}} \qquad [2.17]$$

The notation of the mathematical expectation also applies to the vectors of random variables. We can therefore define the covariance between two random variables as:

$$\begin{aligned} Cov(X_i, X_j) &= E\left[\left(X_i-\overline{x}_i\right)\left(X_j-\overline{x}_j\right)\right] \\ &= \int_{-\infty}^{+\infty}\int_{-\infty}^{+\infty}\left(x_i-\overline{x}_i\right)\left(x_j-\overline{x}_j\right)dx_i\,dx_j \end{aligned} \qquad [2.18]$$

The dimensionless correlation coefficient between two random variables is given by:

$$r_{ij} = \frac{Cov\left(X_i, X_j\right)}{\sqrt{Var\left(X_i\right) Var\left(X_j\right)}} \qquad [2.19]$$

It can be shown that $\left|r_{ij}\right| \leq 1$.

The variables 'X_i' and 'X_j' are referred to as uncorrelated if

$r_{ij} = 0$ (or $Cov\left(X_i, X_j\right) = 0$). Consequently, the statically independent random variables are uncorrelated. However, the zero correlation coefficient (null covariance) does not necessarily involve the static independence of the random variables involved.

The extension of these concepts to the random variable vector $\{X\} = \{X_1, X_2, \rightleftharpoons, X_n\}$ makes it possible to successively define the vector of the mean values and then the covariance matrix:

$$\{\mu(X)\} = \{\bar{x}_1, \bar{x}_2, \rightleftharpoons, \bar{x}_n\} \qquad [2.20]$$

$$\left[\{S(\{X\})\}\right] = \begin{bmatrix} Var\left(X_1\right) & Cov\left(X_1, X_2\right) & \cdots\cdots & Cov\left(X_1, X_n\right) \\ & Var\left(X_2\right) & \cdots\cdots & Cov\left(X_2, X_n\right) \\ sym & & \ddots & \\ & & & Var\left(X_n\right) \end{bmatrix} \qquad [2.21]$$

CENTRAL LIMIT THEOREM.–

Let $\left(X_n\right)$ be a series of independent variables that follow the same probability law with the existence of a common expectation value *m* and a

common variance σ^2 . Then, the centered variable that is associated with the sum $S_n = X_1 + X^2 + \cdots\cdots\cdots\cdots + X_n$, namely $\frac{S_n - mx}{\sigma\sqrt{n}}$, converges to the reduced centered variable (hence of the Gaussian law $N(0,1)$).

2.2.5. *Normal probability functions*

The probability function that is most commonly used in scientific and engineering applications is the normal Gaussian distribution:

$$p(x) = \frac{1}{\sigma(x)\sqrt{2\Pi}} \exp(-\frac{x - \mu(x)^2}{2\sigma(x)^2}) \qquad [2.22]$$

A random variable is referred to as Gaussian (or normal) if its probability density function depends on the mean $\mu(x)$ and the standard deviation $\sigma(X)$ that fully characterizes any Gaussian random variable. A useful expression that is equivalent to equation [1.20] is obtained by defining a new random variable $Y = \frac{X - \sigma(X)}{\sigma(X)}$, which leads to the normalized expression of the Gaussian probability density:

$$p(y) = \frac{1}{\sqrt{2\Pi}} \exp(-\frac{y^2}{2}) \text{ with } \mu(Y) = 0 \text{ and } \sigma(Y) = 1. \qquad [2.23]$$

For a centered Gaussian distribution, the law-generating static moments are given by:

$$E[X^{2n+1}] = 0 \qquad [2.24]$$

$$E[X^{2n}] = \prod_{l=1}^{n} (2l - 1)(\sigma^2)^n \qquad [2.25]$$

with

$$\sigma^2 = E[X^2] = \text{var}(X) \qquad [2.26]$$

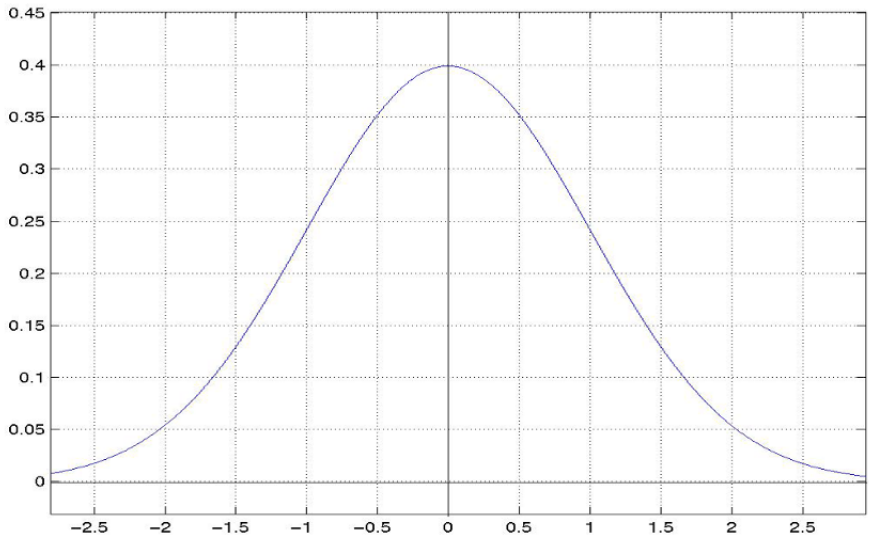

Figure 2.1. *Distribution of the normal law. For a color version of this figure, see www.iste.co.uk/dahoo/metrology1.zip*

The odd powers of the mathematical expectation are therefore null, and the even powers depend on the variance of the random variable.

The Gaussian probability density function has remarkable mathematical properties. It is worth mentioning that the linear functions of Gaussian random variables are also Gaussian.

2.2.6. *Uniform probability function*

The law of a uniform or rectangular probability distribution can be used to characterize random variables whose probability ranges within a specific interval and is proportional to the width of the interval.

Generally speaking, a variable "X" is referred to as a real uniform random variable on the interval [a, b] (where "a" and "b" are two real numbers such that $a \leq b$) if its probability density is defined as:

$$f(x) = \begin{cases} \dfrac{1}{b-a} & \forall x \in [a,b] \\ \\ \text{O} & \forall x \notin [a,b] \end{cases} \qquad [2.27]$$

2.3. Random process and random field

The analysis of many phenomena requires the study of random variables that depend on several parameters.

A random process $\alpha(t,\theta)$ is defined as a parameterized family of random variables for which the index (or parameter) 't' belongs to a set "T" and θ belongs to the space of possible results of the random experiment.

In many engineering problems, the index is time; the fundamental intuitive notion is that of a random variable evolving in time. This is referred to as a random process.

In the presence of several parameters, there is a random field. Random variables are then distributed on a multidimensional space. They represent, for example, the random variation of the thickness of a plate. Therefore, the set of parameters contains spatial coordinates and may contain temporal coordinates.

For a specific value (sample or implementation) of the parameter(s), the value of the field consists of a random variable depending on the considered random phenomenon.

Hence, for a one-dimensional random process $\alpha(t,\theta)$, the result of the random experiment considered can be interpreted in four different ways [DI 00]:

– a family of functions of time (t and θ variable);

– a function of time (t variable, θ fixed);

– a random variable (t fixed, θ variable);

– a number (t fixed, θ fixed).

Let $\alpha(t,\theta)$ be a continuous stochastic field defined on the spatial–temporal coordinates 'x', associated with the "probability space of the random experiment". Since this field is defined in the domain Π of $\Re^d$, we have: $x=\{x_1, x_2, \ldots, x_d\}$.

A vector of random fields $\{\alpha(x,\theta)\}$ can also be defined; therefore, each component is a different random field, although defined by the identical sets of x:

$$\{\alpha(x,\theta)\}=\{\alpha_1(x,\theta),\alpha_2(x,\theta),\ldots,\alpha_P(x,\theta)\} \qquad [2.28]$$

where 'P' is the number of random parameters.

Each vector of random fields $\{\alpha(x,\theta)\}$ is associated with a random parameter of the studied system, and its mean is defined by the spatial mathematical expectation:

$$\mu(\alpha_i(x))=E[\alpha_i(x,\theta)]=\int_{-\infty}^{+\infty}\alpha_i(x,\theta)p_1(\alpha_i(x))d\alpha_i(x) \qquad [2.29]$$

Considering two random fields $\alpha_i(x,\theta)$ and $\alpha_j(x,\theta)$, the covariance can be defined by the following expression:

$$Cov(\alpha_i(x),\alpha_j(x))=\int_{-\infty}^{+\infty}\int_{-\infty}^{+\infty}(\alpha_i(x,\theta)-\overline{\alpha}_i)(\alpha_j(x,\theta)-\overline{\alpha}_j) p_2(\alpha_i(x),\alpha_j(x))d\alpha_i(x)d\alpha_j(x) \qquad [2.30]$$

with $i,j=1,2,\ldots,P$; $p_1(\alpha_i(x))$ being the probability density function of "$\alpha_i(x,\theta)$" and $p_2(\alpha_i(x),\alpha_j(x))$ being the joint probability density

function of $\alpha_i(x,\theta)$ and $\alpha_j(x,\theta)$. The symbol $\overline{\alpha}$ indicates the mean $\mu(\alpha(x))$.

Similar to random variables, the mean and the covariance fully characterize a stochastic field of Gaussian type.

2.4. Mathematical formulation of the model

All the methods described apply to a physical system that has the following properties:

– environment with randomly fluctuating properties;

– random (external) excitation.

This can be expressed by the following equations:

$$\Gamma(x,\theta)u(x,\theta) = f(x,\theta) \qquad [2.31]$$

where Γ is a differential operator that can be rewritten as:

$$\Gamma(x,\theta) = \mathrm{L}(x) + \Pi(\alpha(\theta), x) \qquad [2.32]$$

where L is the deterministic part of Γ and Π is the random part with zero mean.

Knowing Γ and f, the problem is to find the statistical properties of u.

The static properties of the solutions to the problem with eigenvalues associated with the following equation should also be determined:

$$\Gamma(x,\theta)\varphi(x,\theta) = \lambda(x,\theta)\varphi(x,\theta) \qquad [2.33]$$

where $\varphi(x,\theta)$ is the random eigenvector associated with the random eigenvalue $\lambda(x,\theta)$.

2.5. Reliability-based approach

The reliability-based approach involves uncertainty modeling. Depending on the methods used, uncertainties are modeled by random variables, stochastic fields or stochastic processes. These methods are used to study and analyze the variability of the system response and to minimize it.

The most common methods are the Monte Carlo method, the perturbations method and the polynomial chaos method [ELH 13].

2.5.1. *Monte Carlo method*

2.5.1.1. *Origin*

This mathematical tool was first used in 1930 in Fermi's research works on the characterization of new molecules. The Monte Carlo (MC) method was then applied in 1940 by von Neumann, Ulam and Fermi for simulations in atomic physics. The MC method is a powerful and very general mathematical tool. The computational power of current information technology opens a broad field of applications for this method.

2.5.1.2. *Principle*

The MC method is a computation technique that successively solves a deterministic system that incorporates uncertain parameters modeled by random variables.

The MC method is used when the problem is too complex to be solved analytically. It generates random drawings for all the uncertain parameters following their probability laws. The quality in terms of accuracy of random generators is very important. For each drawing, a set of parameters is obtained and a deterministic calculation is made.

2.5.1.3. *Advantages and drawbacks*

The main advantage of the MC method is essentially related to its applicability. This method potentially applies to all systems, irrespective of size or complexity. The results provided are statistically exact, meaning that their uncertainty decreases with the increase in the number of drawings. This uncertainty is defined for a given confidence level by the Bienaymé–Tchebychev inequality. A reasonable accuracy requires a large

number of drawings. This is why the MC method is sometimes very costly in terms of calculation time, which is the major drawback of this method.

2.5.1.4. *Note*

Due to its simplicity, the MC method is applied in the field of engineering sciences. It is a powerful, but costly method. Its results are often used to validate new methods that are developed in fundamental research. It is applied in Chapter 9 of [DAH 16] for the characterization of carbon nanotubes.

2.5.2. *Perturbation method*

2.5.2.1. *Principle*

The perturbation method is another technique for studying the propagation of uncertainties on systems [KLE 92, ELH 13]. It involves the approximation of the functions of random variables by their Taylor expansion about their mean value. Depending on the order of Taylor expansion, the method is referred to as first order, second order or higher order. This method is subjected to the conditions of existence and validity of Taylor expansion, which limit its field of application to cases in which random variables have small dispersions about their mean value [ELH 13, GUE 15a].

The principle of the perturbation method involves the substitution, in the expression of the model response as a function of its parameters, of the random functions by their Taylor expansions. The same order terms are grouped and thus a system of equations is generated. The system is then solved successively, order by order, starting from zero. The mathematical formalism, as well as the general equations, can be found in the work of [ELH 13] and [GUE 15b].

2.5.2.2. *Applications*

There are numerous applications of the perturbation method. It can be used to solve various types of problems related to the propagation of uncertainties under both static and dynamic conditions, and linear and nonlinear conditions. However, good results are obtained only when the uncertain parameters have a low dispersion [ELH 13, GUE 15a].

In the context of vibrational behavior modeling and analysis of the dynamic behavior of systems, [GUE 15b] used the perturbation method for the study of the aerodynamic properties of elastic structures (stacked flat parts) subjected to several uncertain parameters (structural and geometric parameters). This work is the first published application of the stochastic finite element method combined with that of perturbations for the analysis of aerodynamic stability.

In another study, [ELH 13] presented a combination of the method of finite differences with that of perturbations in order to model the vibration problems in uncertain mechanical structures. The method developed is used, as an illustration, to determine the probabilistic moments of frequencies and eigenmodes of a beam whose Young modulus is random.

The second order is generally sufficient to obtain the first two moments with good accuracy. Muscolino [MUS 00] presented a method of dynamic analysis for linear systems with uncertain parameters and deterministic excitations. This method is an improvement of the first-order perturbation technique that sets limits when the dispersion of uncertain parameters is significant. The results obtained are compared to the reference results of the MC method and the second-order perturbation method. A strong correlation is observed between these results.

2.5.2.3. *Note*

The perturbation method relies on the simple principle by which all the random quantities are expressed by their Taylor expansions about their mean values. However, this method is difficult to implement particularly for systems with many degrees of freedom. Moreover, it can only be used when uncertain parameters have low dispersions around their mean values.

EXAMPLE 2.1.– Application of the perturbation method

The objective is to highlight the advantages of the perturbation method proposed by Muscolino in determining the beam response.

Let us consider a beam fixed at both ends, which is freely vibrating in the (Oxy) plane (Figure 2.1).

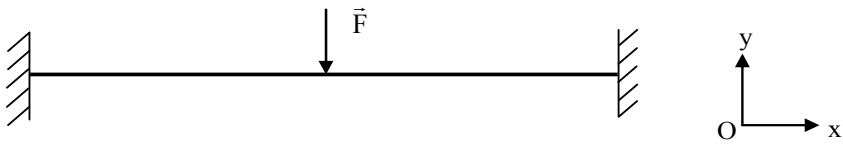

Figure 2.2. *Beam fixed at both ends*

Mass and rigidity matrices are given by:

$$[M]=\frac{m}{420}\begin{bmatrix} 156 & 22.l & 54 & -13.l \\ 22.l & 4.l^2 & 13.l & -3.l^2 \\ 54 & 13.l & 156 & -22.l \\ -13.l & -3.l^2 & -22.l & 4.l^2 \end{bmatrix} \text{s}$$

$$[K]=\frac{E.I}{l^3}\begin{bmatrix} 12 & 6.l & -12 & 6.l \\ 6.l & 4.l^2 & -6.l & 2.l^2 \\ -12 & -6.l & 12 & -6.l \\ 6.l & 2.l^2 & -6.l & 4.l^2 \end{bmatrix} \qquad [2.34]$$

The beam has a square cross-section of edge b that is considered as a Gaussian random variable.

The rigidity matrix [*K*] can be written in the following form:

$[K]= b^4.\ [A]$, where [*A*] is a deterministic matrix.

Similarly, the mass matrix [*M*] can be written as:

$[M]= b^2.\ [B]$, where [*B*] is a deterministic matrix.

Let us study the response of the beam to a force $F= 600\ sin(800t)$ acting at the center of the beam. The mean value and the standard deviation of the shift of the center of the beam are calculated using the second-order perturbation method and the new proposed method. The results obtained are compared to those obtained with the reference Monte Carlo technique using 10,000 drawings.

The results (Figures 2.2 and 2.3) show that the two perturbation methods yield the same results as the MC method.

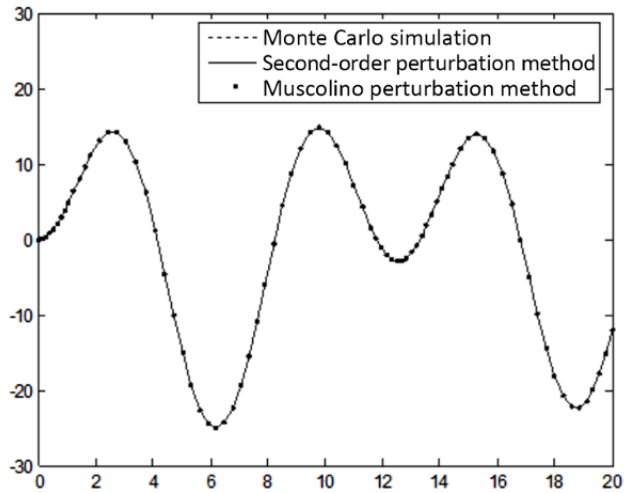

Figure 2.3. *Mean shift of the center of the beam*

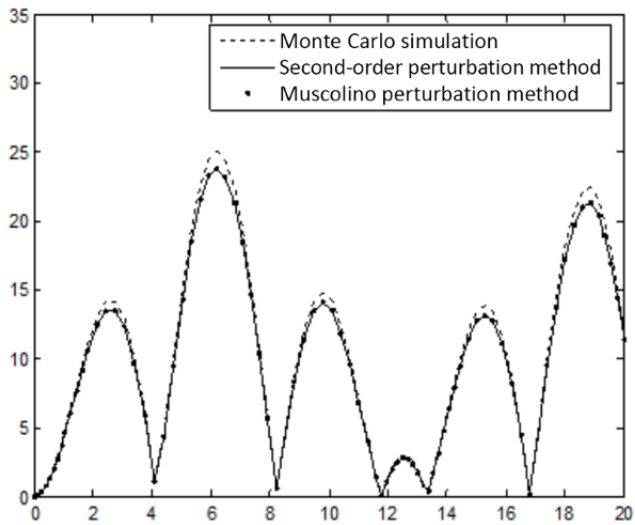

Figure 2.4. *Standard deviation of the center of the beam*

2.5.3. *Polynomial chaos method*

2.5.3.1. *Origins and principle*

The polynomial chaos method is a powerful mathematical tool developed by Wiener in his theory on homogeneous chaos [GUE 15a, GUE 15b]. This method formalizes a separation between the stochastic components of a random function and its deterministic components. Polynomial chaos is used to obtain a functional expression of a random response by decomposing its hazard on the basis of orthogonal polynomials.

Generally speaking, a field of second-order stochastic (finite variance) variables can be expressed by a series expansion of Hermite polynomials; orthogonal functions of certain random Gaussian and independent variables model the uncertainty. The deterministic part is modeled by the coefficients $\overline{x}_j$, known as stochastic modes, weighting the Hermite polynomial functions:

$$X(\xi) = \sum_{j=0}^{\infty} \overline{x}_j \phi_j(\xi) \qquad [2.35]$$

The family of polynomials Φ_i forms an optimal orthogonal basis and enables convergence in the sense of least squares of the expansion [ELH 13]. However, the rapidity of the convergence and the accuracy of the expansion into Hermite polynomials are no longer verified when dealing with non-Gaussian processes. In reality, the optimality of the Hermite basis in the case of Gaussian processes is due to the fact that the probability density function, which in this case is Gaussian, has a mathematical form that is similar to that of the weight function, which is associated with the scalar product defined in the basis. This principle can be generalized and used to establish a correspondence, referred to as the Askey scheme [ASK 85], between the families of orthogonal polynomials and the laws of probability. The notion of expansion into generalized chaos polynomials is then defined. An exponential convergence is thus proven and generalized to the case of random laws of probability (not necessarily Gaussian) [GHA 99].

2.5.3.2. *Note*

Polynomial chaos is a concept well suited to the modeling of random functions and processes. It is a tool for taking into account uncertainties and nonlinearities in system modeling and analysis. The numerical schemes for

the implementation of polynomial chaos-based approaches differ by the way in which they use the model subject to the propagation of uncertainties. The advantage of the intrusive numerical scheme is that it requires only one calculation to determine the stochastic modes. However, this calculation becomes cumbersome when the original model has many uncertain parameters. The calculation complexity becomes more significant in the case of systems that have many degrees of freedom and are strongly nonlinear. This is because the original model is transformed through its projection on the polynomial chaos basis into a system of deterministic equations whose size and complexity depend significantly on the number of uncertain parameters and the number of degrees of freedom of the original model.

However, the non-intrusive scheme has a significant advantage, namely that it does not require modifications or manipulations of the original model. Several applications of this method can be found in [ELH 13].

2.6. Design of experiments method

2.6.1. *Principle*

The design of experiments method is used to implement or simplify, in terms of complexity and costs, an experimental protocol whose objective is to determine the parameters that have an impact on the performance of an industrial product. The purpose of this method is to obtain a design that is not sensitive to the variations of system parameters. By fixing the number of experiments to be conducted, this method makes it possible to determine the influence of several parameters on the responses of the system. Its efficiency when applied to a given system depends on the control of the values to be given to the parameters of the system and on the accuracy of the measurements of the corresponding responses. Several techniques rely on the notion of design of experiments. Various diagrams for building the design of experiments were described by Chatillon [CHA 05].

The use of the Taguchi design of experiments method significantly reduces the number of tests [TAG 86]. This method involves the intersection of two matrices of design of experiments: a control matrix representing adjustable factors and a noise matrix representing noise factors (uncertain parameters). The tests are conducted for combinations of factors that are identified in these matrices. Statistical quantities such as the mean value and

the standard deviation of the response signal are measured. For the evaluation of results, the Taguchi method uses the signal-to-noise ratio and a loss function as the quality criterion. In the version of the method developed by [HUN 05], the notion of orthogonal columns is used for the simultaneous study of several design parameters, which reduces the minimal number of tests.

2.6.2. *Taguchi method*

This statistical method is used to define an experimental protocol whose objective is to render the main response of a system insensitive to various values of its parameters. It involves defining a set of experiments and the various sets of parameters to be used. The number of experiments to be conducted depends on the design parameters that are adjustable, the number of parameters that are variable (uncertain), potential dependences between these parameters and the effect of these parameters on the response (e.g. linear or nonlinear effect).

Considering the variability of many parameters, the Taguchi method makes it possible to optimizer the response of a system. This method originally used the signal-to-noise ratio as a quality index, combining the mean and the variance. The objective of the Taguchi method is to simplify the implementation of the design of experiments. It proposes a choice of matrices of experiments, tools for the choice of the most adapted table and recommendations for considering the interactions between design adjustment factors.

The collections of Taguchi tables serve to:

– choose the matrix of experiments to be developed depending on the number of factors, their modalities and their interactions;

– verify by means of linear graphs that the chosen table takes into account all the factors and their interactions and is a proper representation of the problem being considered;

– know by means of the interaction table the columns where the interactions that were neglected can be found.

EXAMPLE 2.2.– Application of design of experiments to robust design

The objective is to highlight the advantages of the design of experiments method in order to render the response of a system insensitive to the variations of its input variables. Let us consider a microcontroller component inserted in a rectangular printed circuit. The microcontroller component has 256 pins that are connected to the printed circuit by brazing joints. The circuit is fixed in a case made of aluminum alloy by five screws (one in each corner of the circuit and one in the central region of the card). FEM (finite element method) is applied to the card featuring a microcontroller component. The input parameters are the geometrical (position of the fifth screw, thickness of the printed circuit) and physical properties of the materials (printed circuit, brazing, pin, over-molding composite material of the electronic component). The response of the model is the strongest constraint among those exerted on the 256 brazing joints during a heat load.

To retain only the input variables that have a significant effect on the studied response, we focus on a screening design of experiments. When the number of variables is 35, a Plackett–Burman plan is developed. According to this plan, 15 parameters that have an effect on the response are retained.

To obtain the surface of the response, a Latin hypercube (LHS) design of experiments is used for the retained variables. The LHS design involving n tests is the design of experiments for which:

– each parameter has the same number of levels n (the higher this number, the finer the "mesh" and the higher the capacity of the adjusted model to apprehend the optima);

– each parameter has only one level.

When the parameters have different domains of variation, each parameter has n equally distributed levels between its minimum value and its maximum value. The LHS design is suitable for numerical tests due to its simplicity of implementation, as well as because numerical tests do not generate dispersion for the same test. The LHS design is suitable for the spatial interpolation method (Kriging) that is used to obtain the response surface.

The response signal considered is the constraint exerted on the brazing joint of the pin of the microcontroller component, which, among the 256 pins, has the most significant median constraint (a given pin of the

component). Seventy percent of the tests of the LHS design of experiments are used to build the Kriging model. These tests are randomly drawn among the 200 tests. The remaining 30% are used to validate the predictive power of the model.

The resulting response surface makes it possible to approximate the constraint on the brazing joint, which is under the highest constraint among the total of 256. A total of 15 variables are considered in this model of response. To identify the variables with the highest influence on the constraint on the brazing joint, a global sensitivity analysis is conducted among these 15 variables, using the method of Sobol indices. A number of n simulations of input parameters are conducted, and the response is calculated for them (using the Kriging method). Then, in order to study the sensitivity of one of the parameters, a drawing is done once again for all the parameters except this one. This stage is repeated several times by bootstrap. Sobol indices for the studied parameter are then calculated, from the total variance and the variances related to the studied parameter. We obtain a statistical distribution for each index, which is represented as a boxplot, to estimate the confidence interval on the index value.

A total of 1,000 simulations are conducted and thus the input parameters are simulated and 100 indices are calculated. The parameters that have the highest influence on the response are listed below in the order of their importance:

– parameters X1 (COMP_Z): thickness of the brazing joint;

– parameter X4 (EX_SOLDER): Young's modulus of the brazing;

– parameter X5 (ALP_SOLDER): expansion coefficient of the brazing;

– parameter X14 (ALPX COMP): expansion coefficient of the component in the plane.

Once the influencing factors are identified, Monte Carlo simulations are conducted to determine the distribution of the constraint on the brazing joint, depending on the variations of the factors that influence it:

– each non-influencing factor is assigned the nominal value;

– for each influencing factor, a uniform law drawing is done in its field of variation;

– finally, the value of the constraint on the brazing joint is calculated using the Kriging model.

The previously described process is iterated a very large number of times (107), in order to obtain the distribution of the constraint on the brazing joint.

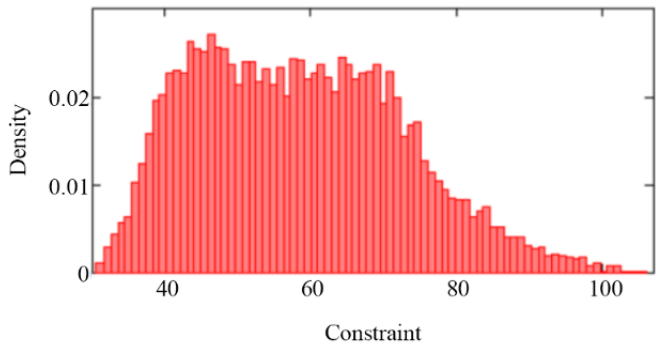

Figure 2.5. *Histogram of the constraint on the brazing joint. For a color version of this figure, see www.iste.co.uk/dahoo/metrology1.zip*

This distribution can be estimated by a parametric model, for example a Gaussian mixture model. The result is presented in Figure 2.5.

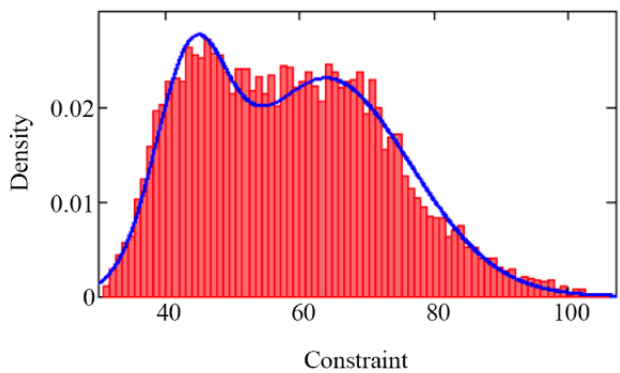

Figure 2.6. *Density of the constraint on the brazing joint. For a color version of this figure, see www.iste.co.uk/dahoo/metrology1.zip*

The objective is to adjust the level of the control factors in order to reduce the sensitivity of the system to the sources of variability (noise factors) and to harmonize the system response with its target (objective).

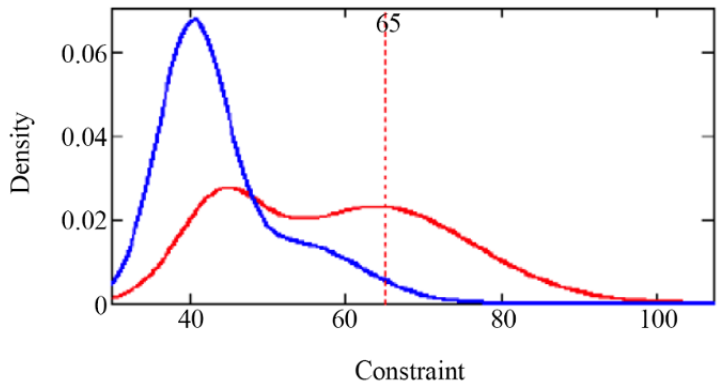

Figure 2.7. *Density of the initial constraint (red) and the optimized constraint (blue). For a color version of this figure, see www.iste.co.uk/dahoo/metrology1.zip*

Factor ALPX COMP (CTEX of the component) has a strong influence on the constraint (positive influence). This factor can be adjusted by the composite structure of the component coating material. Small values of ALPX COMP should be drawn to minimize the constraint. By initially reducing the range of variation of factor ALPX COMP to the interval [5;7], instead of [5;23], the mean value of the constraint is reduced, as well as its variability (Figure 2.6).

2.7. Set-based approach

The prerequisite of the above-described reliability-based approach is that the laws of probability governing the uncertain parameters are known. The advantage of the set-based approach is that it does not require models of the laws of probability of uncertainties. Two significant methods are found in the set-based approach: the first is based on interval arithmetic [MOO 66]; the second is based on the fuzzy logic formalism [ZAD 65].

2.7.1. *The interval method*

2.7.1.1. *Principle*

Interval calculation is rooted in the works of Moore [MOO 66]. This method relies on modeling uncertain parameters by intervals whose endpoints represent the minimal and maximal limits of the parameters. It can then be considered that the error between the model output and the system response is bounded and the endpoints are known. These endpoints take into account the measurement noise and modeling errors. The objective is to find a set of acceptable values instead of one value of the parameters, minimizing a convergence criterion. This method can be readily used. In contrast to probabilistic methods, no information is required on the nature of dispersions or on the way in which they evolve. However, it presents convergence difficulties.

2.7.1.2. *Interval arithmetic and stability analysis*

Interval arithmetic is applied to the analysis and stability of uncertain linear dynamic systems. Jaulin *et al.* [JAU 01] proposed a method for the characterization of all the values of uncertain parameters associating a stable dynamic behavior. For the study of stability, the solution is determined using the interval-based analysis according to the Routh criterion. Defining two sets A and B, stability analysis boils down to an inclusion problem. A is the admissible set of possible values of uncertain parameters, while B is the admissible set of values for which the system is stable. An algorithm based on the theory of intervals can be used to test the inclusion of A in B synonymous with a necessary and sufficient condition that proves the stability. The convergence of the algorithm is tested on numerical examples of systems.

EXAMPLE 2.3.– Interval method: vehicle suspensions

An example of application is a mass–spring–shock absorber system (Figure 2.7). This system is defined by the following equations:

$$\begin{cases} \dot{x}_s = v_s \\ \dot{x}_u = v_u \\ \dot{v}_s = -\dfrac{1}{m_s}\left(c_s\left(\dot{x}_s - \dot{x}_u\right) + k_s\left(x_s - x_u\right) + K_s\left(x_s - x_u\right)^3\right) \\ \dot{v}_u = -\dfrac{1}{m_u}\left(c_s\left(\dot{x}_s - \dot{x}_u\right) + k_s\left(x_s - x_u\right) + K_s\left(x_s - x_u\right)^3 - k_t\left(x_u - x_r\right) - K_t\left(x_u - x_r\right)^3\right) \end{cases} \quad [2.36]$$

where m_s and m_u are the masses, c is the damping coefficient, k_s and k_t are the linear rigidities, K_s and K_t are the cubic rigidities.

The initial conditions are:

$$[x_s, x_u, v_s, v_u]\big|_{t=0} = [0,0,0,0].$$

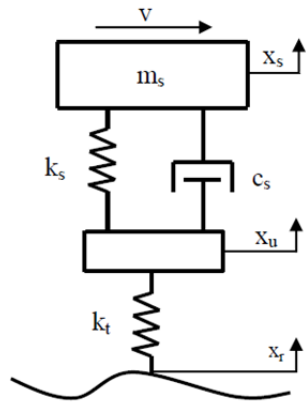

Figure 2.8. *Mass–spring–shock absorber system*

The parameters c_s, k_s and k_t are uncertain and modeled by intervals, as indicated in Table 2.1.

Parameters	m_s(kg)	C_s(Ns/m)	K_s(Ns/m)	K_t(Ns/m)	K_s(N/m^3)	K_t(N/m^3)
Mean value	375	1000	15000	200000	$1.5*10^6$	$2*10^7$
Interval	-	[900,1100]	[13500,16500]	$[18,22]*10^4$		

Table 2.1. *Parameters of the mass–spring–shock absorber system model*

The mean value of the shift is calculated using the interval method. The result (Figure 2.8) is compared to that obtained by the deterministic method. There is an agreement between the result of the interval method and that of the deterministic method.

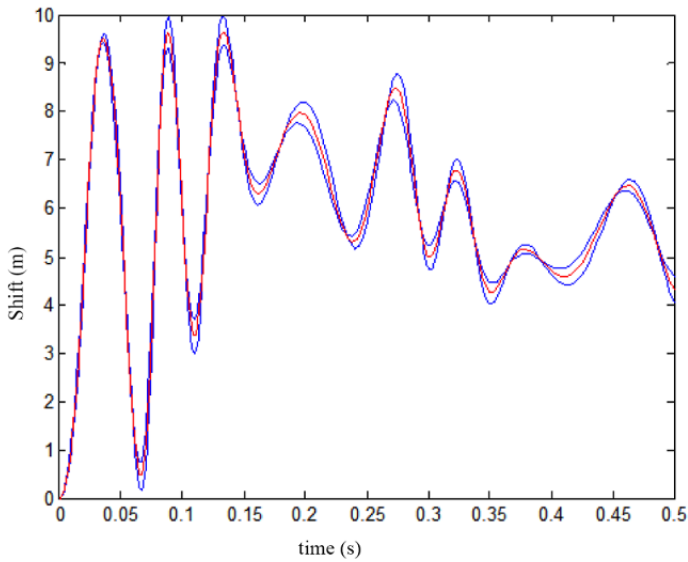

Figure 2.9. *Mean value of the shift xu(t) for the interval method (blue) and the deterministic method (red). For a color version of this figure, see www.iste.co.uk/dahoo/metrology1.zip*

2.7.1.3. *Conclusion*

Interval arithmetic can be used for modeling uncertainties only through their physical boundaries, which in most cases are identifiable and measurable. No information is required on the evolution of uncertainty in its interval.

2.7.2. *Fuzzy logic-based method*

2.7.2.1. *Principle*

The methods based on fuzzy logic were introduced for the interpretation and manipulation of uncertain data when no probabilistic or statistical information is available. These methods rely on the notion of a fuzzy set. An element of the fuzzy set, such as a model input value, has a degree of belonging to this set. This notion, which is formally known as the function of belonging, differs from the notion of probability. It defines an evasive quantitative measure of imperfect data. According to this definition, it is

possible to establish a fuzzy logic associated with degrees of freedom, which, assigned to propositions, range from zero (false) to one (true) with all the possible graduations, leading to the following terms: a little, moderately, etc. Fuzzy logic can thus be applied to approximate reasoning.

EXAMPLE 2.4.–Application of the fuzzy logic-based method

Let us consider the application example of a two-dimensional frame under free vibration. This system, which is represented in Figure 2.9 in the (OXY) plane, consists of three beams of equal square section a. The only random parameter is the dimension a. The objective is to determine the stochastic shift of the horizontal beam of the frame during a given sinusoidal excitation ($F(t)$):

$$F(t) = 20\ sin(80t)$$

The mean value and the standard deviation of the shift are calculated using the fuzzy logic-based method. The results (Figures 2.10 and 2.11) are compared to those of the reference method (Monte Carlo). It can be noted that the stochastic response of the frame (mean value and standard deviation of the shift of the beam) calculated by the fuzzy logic-based method is in agreement with the response calculated by the MC method.

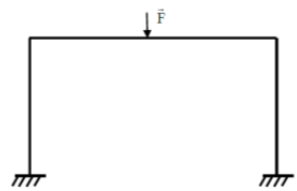

Figure 2.10. *Two-dimensional frame*

2.7.2.2. *Conclusion*

The fuzzy logic-based method for considering uncertainties can be used for dealing with vague, imprecise or linguistically described information. This uncertainty is described by form functions referred to as functions of belonging. The main advantage of this modeling is that it does not require statistical or probabilistic information. However, it is difficult to determine the function of belonging.

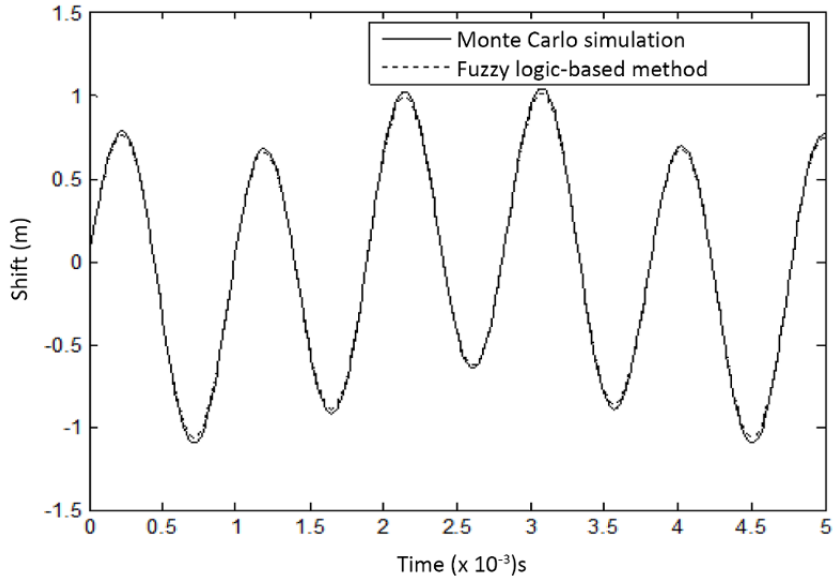

Figure 2.11. *Mean value of the shift as a function of time*

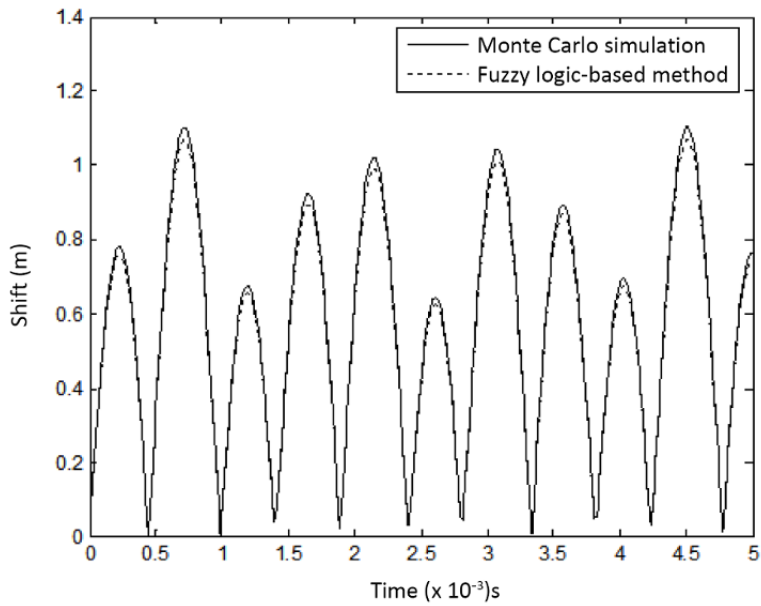

Figure 2.12. *Standard deviation of the shift as a function of time*

2.8. Analysis in terms of main components

The objective of this method is to determine the most significant components of a system depending on several variables. For example, a sample of N individuals characterized by P characters (or variables) is analyzed. The many relations between N and P will be analyzed.

In order to analyze the connection between two variables, their values are plotted on two orthogonal axes and the effect of these variables is analyzed using statistical tests. For three variables, this approach leads to a three-dimensional graphical representation. For four or more variables, the graphical representation is no longer possible. If the work is conducted on pairs or triplets of variables, complex interactions risk remaining hidden, which leads to the necessity of implementing a technique that extracts the most relevant information. This technique uses linear combinations of variables and is adapted to linear relations.

2.8.1. *Description of the approach*

Let X_1, X_2,... X_p be the initial quantitative and centered variables (of zero mean). A new variable Y_1 is determined as a linear combination of X_i:

$$Y_1 = c_1 X_1 + c_2 X_2 + ... + c_p X_p \qquad [2.37]$$

where c_1, c_2, …, c_p are constants to be determined, such that Y_1 has a maximum variance with the following constraint:

$$c_1^2 + c_2^2 + ... + c_p^2 = 1 \qquad [2.38]$$

Among all the linear combinations of X_i, the one that generates the least possible destruction of information has the widest possible dispersion. If Y_1 has zero dispersion, Y_1 is a constant. The problem to be solved is to determine the constants c normed to 1 for which the variance of Y_1 is maximal. The constants c (and therefore Y_1) can be determined. The variable Y_1 is referred to as the main component and V_1 is its variance.

In general, Y_1 does not exhaust all of the variance of the original variables. Then, a second variable Y_2 is determined, not correlated with Y_1, of maximum variance, as a linear combination of X_i:

$$Y_2 = c_{12}X_1 + c_{22}X_2 + ... + c_{p2}X_p \quad [2.39]$$

where c_{12}, c_{22}, …, c_{p2} are constants to be determined under the normalization constraint:

$$c_{12}^2 + c_{22}^2 + ... + c_{p2}^2 = 1 \quad [2.40]$$

NOTE.–

It is possible to replace c_{11} with c_1 and c_{21} with c_2, etc. It can then be proven that the constants c (and hence Y_2) are uniquely determined.

Let V_2 be the variance of the new variable Y_2. By construction, we have: $V_1 \geq V_2$.

Y_2 is referred to as the second main component. New variables Y_3, Y_4,…,Y_p can be built in a similar manner. These variables are not correlated with the previous ones, of maximum variance (the normalization condition being related to the coefficients of the linear combination).

Let V_3, V_4,…,V_p be the variances of these new variables. We then have:

$$V_3 \geq V_4 \geq V_5 ... \geq V_p \quad [2.41]$$

2.8.2. *Mathematical basis*

Determining constants c (or those of Y) amounts to determining eigenvalues. The various c are the coordinates of (normed) eigenvectors of the variance–covariance matrix of the initial variables X. The variances V_1, V_2,…,V_p are the associated eigenvalues. The various cited properties (existence and uniqueness) can be deduced from them. If the r^{th} variance V_{r+1} is very small, variables Y_{r+1}, Y_{r+2},…,Y_p are approximately constant for all the individuals. Keeping only the main components, Y_1, Y_2,…,Y_p is therefore natural. In practice, V_{r+1} is estimated to be small if:

$$\frac{(V_1 + V_2 + ... + V_r)}{(V_1 + V_2 + ... + V_p)} \approx 90\% \quad [2.42]$$